Journal of Cranio-Maxillo-Facial Surgery 47 (2019) 473–483

Contents lists available at ScienceDirect

Journal of Cranio-Maxillo-Facial Surgery

journal homepage: www.jcmfs.com

Investigation of the effects of semaphorin 3A on new bone formation in a rat calvarial defect model☆

Sevinç Kenan [a, *], Özen Doğan Onur [a], Seyhun Solakoğlu [b], Tuğba Kotil [b], Mustafa Ramazanoğlu [a], Hakan Hamdi Çelik [c], Mert Ocak [c], Bora Uzuner [c], Erhan Fıratlı [d]

[a] Department of Oral and Maxillofacial Surgery (Head: Prof. Dr. Hülya Koçak Berberoğlu), Faculty of Dentistry, Istanbul University, Istanbul, Turkey
[b] Department of Histology and Embryology (Head: Prof. Dr. Seyhun Solakoğlu), Faculty of Medicine, Istanbul University, Istanbul, Turkey
[c] Department of Anatomy (Head: Prof. Dr. M. Fevzi Sargon), Faculty of Medicine, Hacettepe University, Ankara, Turkey
[d] Department of Periodontology (Head: Prof. Dr. Serdar Çintan), Faculty of Dentistry, Istanbul University, Istanbul, Turkey

ARTICLE INFO

Article history:
Paper received 15 May 2018
Accepted 17 December 2018
Available online 20 December 2018

Keywords:
Semaphorin 3A
Calvarial bone defect
Bone regeneration

ABSTRACT

Purpose: This study investigates the effects of semaphorin 3A on new bone formation in an experimental rat model.

Materials and methods: Cortical bone defects, 5 mm, were created in the calvaria of 40 Wistar rats, which were then separated into three groups: empty defect (control) group, collagen group, collagen + semaphorin 3A group. The bone blocks were harvested after 4 and 8 weeks. New bone formation was assessed by micro-computed tomography (micro-CT), histology, histomorphometry, transmission electron microscope (TEM) and immunohistochemistry.

Results: Increased bone formation was observed in collagen + semaphorin 3A groups both histologically and with micro-CT. In the histomorphometic analysis, the control group had significantly less bone formation compared to both the collagen and collagen + semaphorin 3A group at 4 weeks ($p = 0.0001$) and 8 weeks ($p = 0.0001$). The collagen group had significantly less bone formation compared to collagen + semaphorin 3A group both at 4 weeks ($p = 0.002$) and 8 weeks ($p = 0.005$). Immunohistochemical analysis revealed that semaphorin 3A inhibited receptor activator of nuclear factor-kB ligand (RANKL) expression and increased the expressions of osteoblastic bone markers at 4 weeks. In TEM analysis, the collagen + semaphorin 3A group had an increased proliferation and bone formation rate at 4 weeks, whereas bone quantity and maturation were enhanced at 8 weeks.

Conclusion: Locally applied semaphorin 3A increases callus formation at 4 weeks and bone formation at 8 weeks. Semaphorin 3A prevents bone resorption by inhibiting osteoclasts and increases bone formation by inducing osteoblasts.

1. Introduction

Regeneration of bone defects in the maxillofacial region caused by trauma, infection, tumors or genetic disorders is a clinical challenge that usually requires a bone grafting procedure. Autologous bone, which can be harvested from mandibular symphsis, ramus, iliac crest or tibia, is considered the gold standard for bone regeneration. Yet, it has important disadvantages, such as having a limited bone supply and donor site morbidity. Various biomaterials and bone substitutes have been developed to overcome the disadvantages associated with harvesting autogenous bone and to increase bone repair. Osteoinductive biomaterials, such as bone morphogenic proteins and various growth factors, are being constantly investigated to enhance bone regeneration in compromised bone defects (Stancoven et al., 2012; García-Gareta et al., 2015; Shah et al., 2015).

Bone tissue is continuously being broken down and then rebuilt throughout life by a process called remodeling. This process, which

☆ This study was supported by the 3001- Research and Development Projects Funding Program of the Turkey Scientific Technology Research Foundation (TUBITAK) (Project No: 214S554).

* Corresponding author. Fax: +0090 212 531 2230.
E-mail address: sevinckenan85@gmail.com (S. Kenan).

https://doi.org/10.1016/j.jcms.2018.12.010
1010-5182/

is crucial for the maintenance of both bone quality and strength, requires a dynamic interaction among bone cells including osteoclasts, osteoblasts and osteocytes. Coupling between bone resorption and formation is essential for the homeostasis of the skeletal system. Recent advances have shown that bone remodeling is regulated by various molecules that mediate communication among bone cells (Negishi-Koga; Takayanagi, 2012). There is also evidence that neuronal regulation is important for bone metabolism (Gomez et al., 2005; Zhang et al., 2013). Recently, a protein named semaphorin 3A has been implicated in the regulation of bone remodeling both directly and indirectly via neural control (Xu, 2014).

Semaphorins are a large family of secreted or transmembrane proteins which were originally identified as molecules that control axon pathfinding during the development of the nervous system. More than 20 types of semaphorins have been discovered, and these proteins have been associated with diverse functions in many biological processes, including cardiogenesis, angiogenesis, oncogenesis and regulation of immune responses (Yazdani; Terman, 2006; Roth et al., 2009; Jongbloets; Pasterkamp, 2014; Epstein et al., 2015). Recent findings suggest that semaphorin molecules are also involved in bone homeostasis and various bone disorders (Kang; Kumanogoh, 2013; Verlinden et al., 2016).

Semaphorin 3A is an axonal guidance protein belonging to the semaphorin family, which was first identified as an axonal chemorepellent. Besides the nervous system, semaphorin 3A has multifunctional roles in embryonic development, immune regulation, vascularization, and oncogenesis (Xu, 2014). Recent studies have demonstrated the importance of Semaphorin 3A and its receptors, neuropilin-1 (Nrp1) and plexin A, in the skeletal system. Semaphorin 3A-deficient mice were shown to have abnormal bone development. Behar et al. (1996) reported that semaphorin 3A-deficient mice displayed fusion of cervical bones, partial duplication of ribs, and poor alignment of the rib–sternum junctions. Semaphorin 3A-deficient mice also had a severe osteopenic phenotype (Hayashi et al., 2012; Fukuda et al., 2013).

A recent study has shown that semaphorin 3A exerts a dual osteoprotective effect by suppressing osteoclastic bone resorption and increasing osteoblastic bone formation simultaneously. It is demonstrated that the binding of Semaphorin 3A to Nrp1 inhibits receptor activator of nuclear factor-kB ligand (RANKL)-induced osteoclast differentiation by inhibiting the immunoreceptor tyrosine-based activation motif (ITAM) and RhoA signaling pathways. This binding is also shown to stimulate osteoblastic differentiation and to inhibit adipocyte differentiation through the canonical Wnt/β-catenin signaling pathway (Hayashi et al., 2012).

Osteostimulative effects of semaphorin 3A can be utilized to promote the repair of bone defects, to enhance bone regeneration in implant surgery and to increase osteointegration of titanium implants (Fang et al., 2014; Liu et al., 2016; Li et al., 2017). The fact that semaphorin 3A promotes bone regeneration by reducing bone resorption and increasing bone formation simultaneously could also lead to new therapeutic agents for the treatment of various bone disorders, including osteoporosis (Zaidi; Iqbal, 2012). The mechanism of action of semaphorin 3A is different from those of current therapeutic interventions in osteoporosis, since current therapies generally reduce bone turnover instead of balancing impaired bone turnover (Harre; Schett, 2013).

The purpose of this study is to observe the effects of semaphorin 3A on bone remodeling and regeneration. For this purpose, critical-size defects were formed in the rat calvaria, and semaphorin 3A was applied locally using a collagen matrix carrier. The effects of semaphorin 3A on osteoblastic bone formation and osteoclastic activity were observed using various investigation methods, including histology, immunohistochemistry, and transmission electron microscope (TEM) analysis. The amount of newly formed bone was assessed by micro-computed tomography (micro-CT) and histomorphometric analysis.

2. Materials and Methods

2.1. Experimental design and surgical procedures

In the present study, a total of 40 male Wistar rats, aged 12 weeks with an average weight of 300–350 g, were used. The experimental protocol was approved by the Animal Experiments and Ethics Committee of Istanbul University (no: 127/2013). The animals were anesthetized by intramuscular injection of 40 mg/kg ketamine (Ketalar, Pfizer, Istanbul, Turkey) and 8 mg/kg xylazine (Alfazyne, 2%, Alfasan, Woerden, Holland). After the surgical site was shaved and scrubbed with iodine, additional local anesthesia with lidocaine (Jetokain, Adeka, Samsun, Turkey) was applied. An incision was made in the scalp in the sagittal plane across the cranium, and a full-thickness flap was elevated. A 5-mm critical-sized bone defect was made in the right side of the calvarium with a trephine bur, with an outer diameter of 5 mm (Meisinger, 229-040 RAL, USA), without harming the dura mater and under continuous irrigation with sterile saline.

The animals were randomized into three study groups: control group (n = 8), collagen group (n = 16) and collagen + semaphorin 3A group (n = 16). The bone defect was left empty in the control group. Socket preserving cones of type 1 collagen (Parasorb Cone, Resorba Medical GmbH, Nurnberg, Germany) were cut into round pieces using a tissue punch (Meisinger, 225RF/040, USA), 5 mm in diameter, with a surgical handpiece. The prepared collagen matrices were placed into the bone defects in the collagen group. For the third group, collagen matrices with recombinant rat semaphorin 3A (Mybiosource, San Diego, CA) were applied into the defect (Fig. 1). The semaphorin dosage was calculated as 0.5 mg/kg of body weight, based on recent literature (Hayashi et al., 2012).

The wound was closed primarily with 4.0 silk sutures and the rats were given postoperative 30 mg/kg ceftriaxone (Rocephin, Roche, Istanbul, Turkey) for three days. The animals were kept in cages in pairs and received water and food ad libitum.

2.2. Animal sacrifice and specimen collection

Half of the rats of each group (n = 20) were sacrificed after 4 weeks and the remaining half (n = 20) were sacrificed after 8 weeks. At the end of the observation period, the rats were euthanized by using 150 mg/kg sodium pentobarbital (Pentothal Sodium, Abbott, Istanbul, Turkey) and the calvarial bone blocks were harvested. The area of the original surgical defect was removed with the surrounding sound bone using a trephine bur 10 mm in diameter (Meisinger, 229-100 RAL, USA) (Fig. 1).

One bone block from each group was spared for micro-CT analysis, and these blocks were fixed in 10% neutral formalin. A thin slice was cut from each of the remaining blocks and placed in glutaraldehyde solution for TEM analysis. The remaining specimens were fixed in 10% neutral formalin and were prepared for histological and immunohistochemical analysis.

2.3. Micro-CT assessment

Six specimens, each representing a study group, were scanned on a micro-CT system (Skyscan 1174, Skyscan, Kontich Belgium). The specimens were fixed and the scanning system was set to

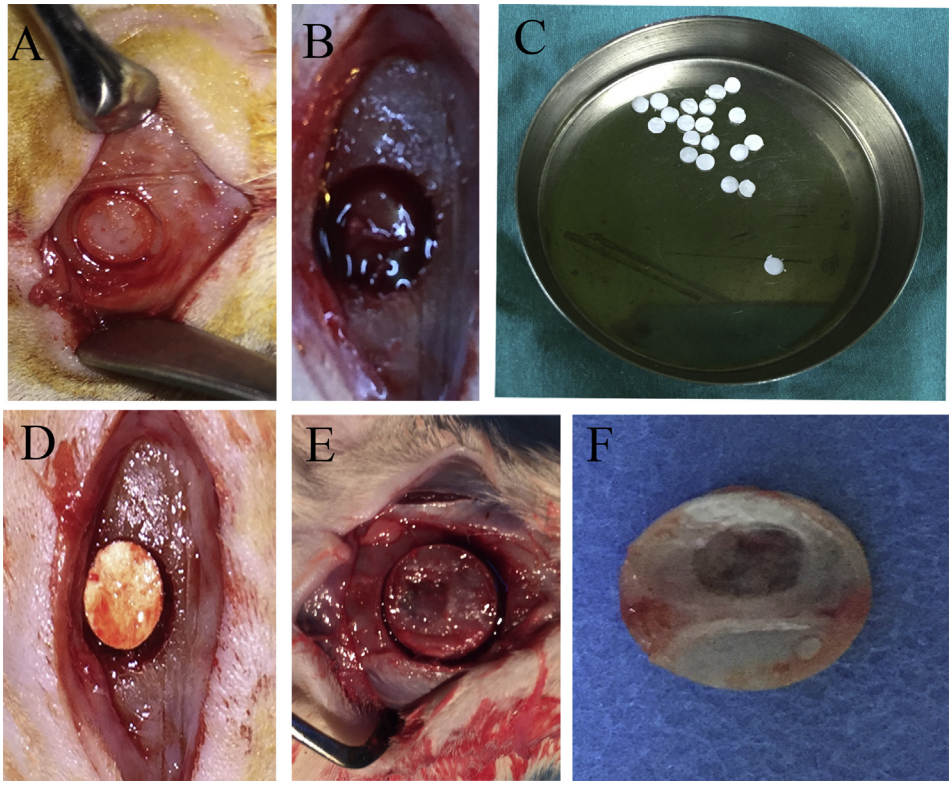

Fig. 1. (A) Osteotomy made in the right side of the calvarium using a 5-mm trephine bur. (B) Image of the 5-mm calvarial bone defect. (C) Type I collagen matrices prepared with a 5-mm tissue punch. (D) Application of the collagen matrix with or without semaphorin 3A to the osteotomy defect. (E) Osteotomy made with a trephine bur, 10 mm in inner diameter, for harvesting the calvarial bone after 4 and 8 weeks. (F) Harvested 10-mm bone blocks including the original bone defect.

50 kV, 800 μA, 40.89 μm pixel size and 2300 ms exposure time. Each specimen was scanned approximately for 1 h. Reconstruction of the scanned data was performed using Nrecon (version 1.6.9.4, Skyscan, Kontich, Belgium) and the reconstructed 8-bit grey images were analyzed with CTAn software (version 1.13.5.1) program.

The region of interest (ROI) was selected by identifying the upper and lower limits of the defect area. Basic parameters were quantified within the ROI, including bone volume (BV), tissue volume (TV) and percent bone volume (BV/TV).

2.4. Histological and histomorphometric analysis

The blocks fixed in 10% neutral formalin were decalcified in 5% formic acid for 2 days. After decalcification, the specimens were dehydrated in graded ethanol (70%, 90%, 96%, %100) for 1 day per each concentration. Next, the blocks were embedded in paraffin and sectioned at 4 μm using a Leicha RM2255 microtome (Leicha, Nussloch, Germany). The sections were stained with hematoxylin–eosin (H&E) for analysis by light microscopy. Olympus Soft Imaging Solutions–Image Analysis software (Olympus Soft Imaging Solutions GmbH, Münster, Germany) was used for the histomorphometric analysis. The digitalized images were analyzed, and the area of the newly formed bone compared to the total area of the defect was measured.

2.5. TEM analysis

The specimens were kept in 2.5% glutaraldehyde solution (Merck, Darmstadt, Germany) at 40 °C for TEM analysis. After they were treated with phosphate-buffered saline solution for 10 min, they were kept in 1% osmic acid for 1 h at 40 °C. After treatment with phosphate-buffered saline solution for 2 × 10 min, they were kept in 1% uranyl acetate at 40 °C for 1 h and treated with phosphate-buffered saline solution for 10 min. The specimens were passed through several steps of alcohol for dehydration. Next, the specimens were first kept in propylene oxide for 2 × 10 min, then in propylene oxide-epon mixtures (1:1 and 1:3) for 1 h each and finally in pure epon (Sigma, 45359) for 1 h at room temperature. The blocks were formed in epon capsules by incubating for 18 h at 600 °C. The prepared blocks were sectioned using ultra-microtome (Leica, EM UC7, Germany) first into semi-thin sections of 0.5 μm, then into thin sections 40–60 nm in thickness. The sections were treated with uranyl acetate for 30 min and lead nitrate for 10 min. They were then analyzed and photographed using TEM (JEOL, JEM-1011), MegaView imaging system and AnalySIS software (Soft Imaging Software). Structural and morphological examination of the defect area was performed by TEM. Cellular arrangements and surface properties were also evaluated.

2.6. Immunohistochemistry

The prepared sections were incubated at 56 °C overnight in order to melt paraffin. The sections were treated with toluene twice for 30 minutes and then passed through several concentrations of alcohol and finally treated with distilled water. Next they were incubated with 5% hydrogen peroxide solution (in methanol) for 13 min in darkness to inhibit endogen peroxidase activity and then washed with buffer solution. The sections were incubated three times with citrate buffer for 5 min and then left to cool for 20 min.

Ultra V block (TA-060-UB) in the Ultravision detection system anti-polyvalent HRP kit was used to prepare blocks. Primary antibodies were applied overnight with a dilution ratio of 1/1000.

Next, the sections were treated with goat anti-polyvalent seconder antibody (TP-060-BN) for 10 min, followed by streptavidin peroxidase (TS-060-HR) for 10 min at room temperature. Ultravision detection system AEC Substrate system – TA-125-HA chromogen was applied for specified durations for each antibody.

Immunohistochemical localizations of receptor activator of nuclear factor-kB (RANK), RANKL, osteoprotegerin (OPG), runt-related transcription factor 2 (Runx2), osterix/SP7, β-catenin and activating transcription factor 4 (ATF4) were carried out using commercially available antibodies according to the manufacturer's suggested protocol. Stained sections were examined qualitatively under light microscopy with a digital camera. Immunoreactivity was assessed and evaluated as none (−), slight (+), medium (++) and strong (+++).

2.7. Statistical analysis

Data are expressed as mean ± standard deviation. Statistical analyses were performed using NCSS (Number Cruncher Statistical System) 2007 Statistical Software (NCSS LLC, Kaysville, UT) program. Multiple comparisons between groups were carried out using one way analysis of variance, and the Tukey test was used for subgroup comparisons. An independent-samples t-test was used for the comparisons of two means. $P < 0.05$ was considered statistically significant.

3. Results

3.1. Micro-CT evaluation

The amount of new bone formation is shown in the representative micro-CT images of each study group (Fig. 2). Quantitative results of micro-CT analysis are expressed as BV/TV. At 4 weeks, BV/TV values were found to be 16.97% for the control group, 28.47% for the collagen group and 33.21% for the collagen + semaphorin 3A group. At 8 weeks, BV/TV values were 49.58% for the control group, 60.96% for the collagen group and 77.10% for the collagen + semaphorin 3A group.

Radiographically, both the collagen and collagen + semaphorin 3A group showed enhanced bone formation compared to the control group at 4 and 8 weeks. The most enhanced bone formation was detected in 8 week collagen + semaphorin 3A group. Quantitatively, this group also displayed the highest bone volume percentage.

3.2. Histological and histomorphometric analysis

Histological representations of the decalcified bone specimens from the experimental groups are shown in Fig. 3. At 4 weeks, a thin uninterrupted bone is observed in the defect area of collagen + semaphorin 3A group, whereas mostly fibrous connective tissue is found in the other two groups at 4 weeks. At 8 weeks, the highest amount of lamellar bone formation and nearly complete defect closure were found in the collagen + semaphorin 3A group. At 8 weeks, the defect area of control group displayed mostly fibrous connective tissue with random ossification foci. Compared to the 8-week control group, the 8-week collagen group showed significantly more ossification sites.

In the histomorphometric analysis of the histological sections, percentage bone formation values (bone area/total area ×100, %) of the groups at 4 weeks were found as 15.12% ± 11.69% for the control group (n = 19), 27.17% ± 5.60% for the collagen group (n = 22) and 32.411% ± 4.95% for the collagen + semaphorin 3A group (n = 18). At 8 weeks, percentage bone formation values were 48.18% ± 5.26% for the control group (n = 26), 67.44% ± 5.31% for the collagen group (n = 19) and 74.46% ± 9.41% for the collagen + semaphorin 3A group (n = 22).

Statistically significant differences in percentage bone formation values were found between the groups at 4 weeks (p = 0.0001). At 4 weeks, the control group exhibited significantly lower percentage of bone formation compared to the collagen group and the

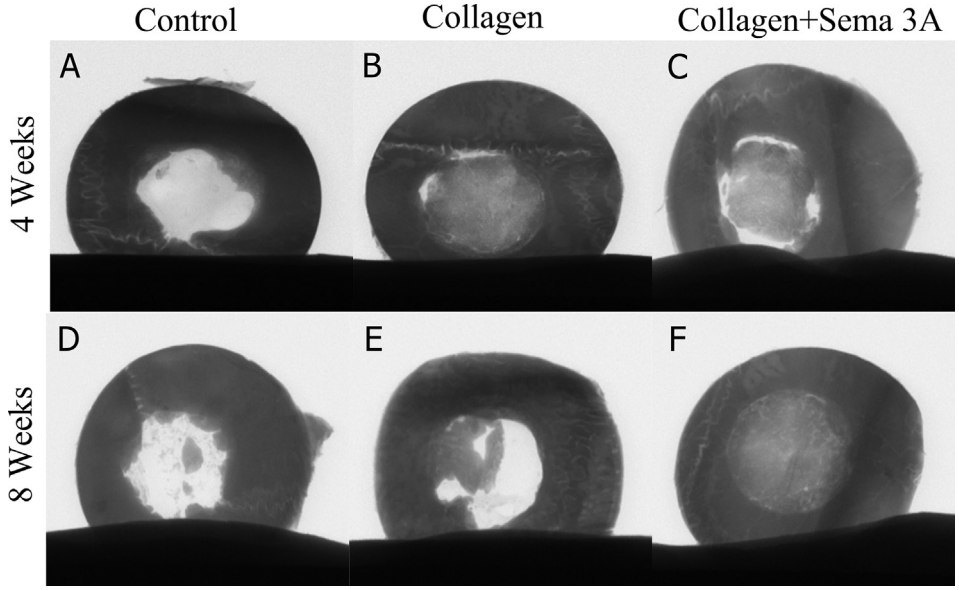

Fig. 2. (A) Micro-CT image from control group at 4 weeks. (B) Micro-CT image from collagen group at 4 weeks. (C) Micro-CT image from collagen + semaphorin 3A (Sema3A) group at 4 weeks. (D) Micro-CT image from control group at 8 weeks. € Micro-CT image from collagen group at 8 weeks. (F) Micro-CT image from collagen + semaphorin 3A group at 8 weeks. The most enhanced bone formation is observed in this group, as the bone defect is almost completely filled with new bone.

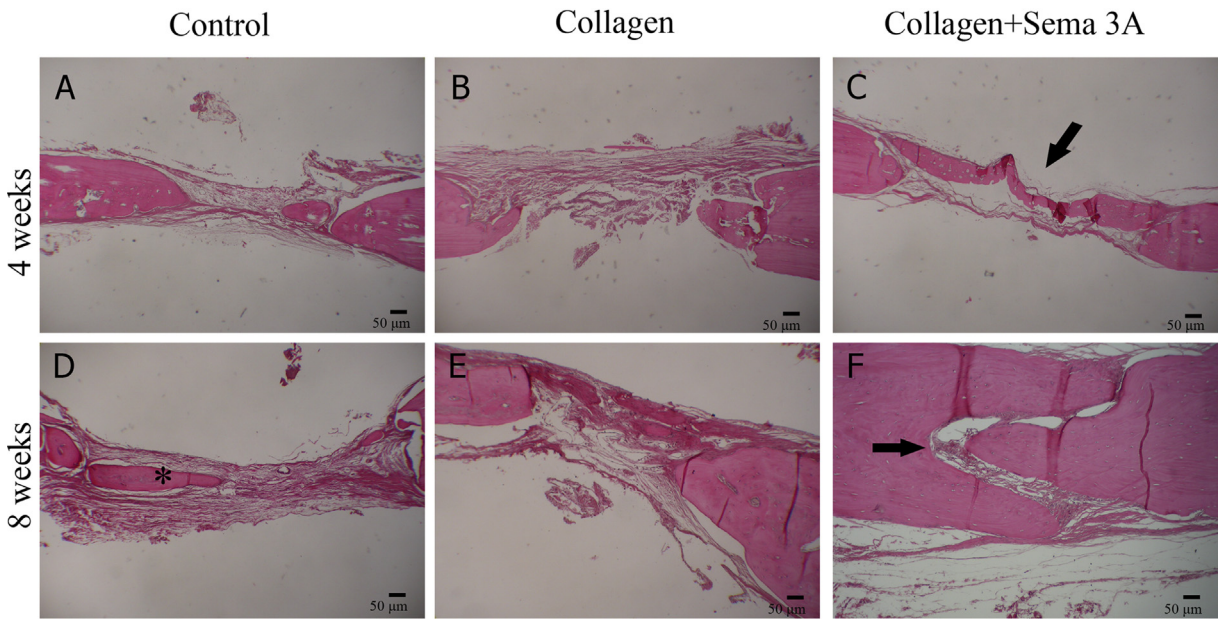

Fig. 3. (A) Light micrograph from control group at 4 weeks. (B) Light micrograph from collagen group at 4 weeks. (C) Light micrograph from collagen + semaphorin 3A (Sema3A) group at 4 weeks. Arrow indicates the uninterrupted new bone formation in the osteotomy defect. (D) Light micrograph from control group at 8 weeks. Asterisk indicates mostly connective tissue with new ossification foci. E, Light micrograph from collagen group at 8 weeks. More ossification sites are observed compared to the 8-week control group. (F) Light micrograph from collagen + semaphorin 3A group at 8 weeks. Arrow indicates the thin suture formation between newly formed lamellar bone. Scale bar = 50 μm, original magnification ×150.

collagen + semaphorin 3A group ($p = 0.0001$). At 4 weeks, the collagen group had a significantly lower percentage of bone formation compared to the collagen + semaphorin 3A group ($p = 0.002$).

The differences in percentage of bone formation values between the groups at 8 weeks were statistically significant ($p = 0.0001$). At 8 weeks, the control group exhibited a significantly lower percentage of bone formation compared to the collagen group and the

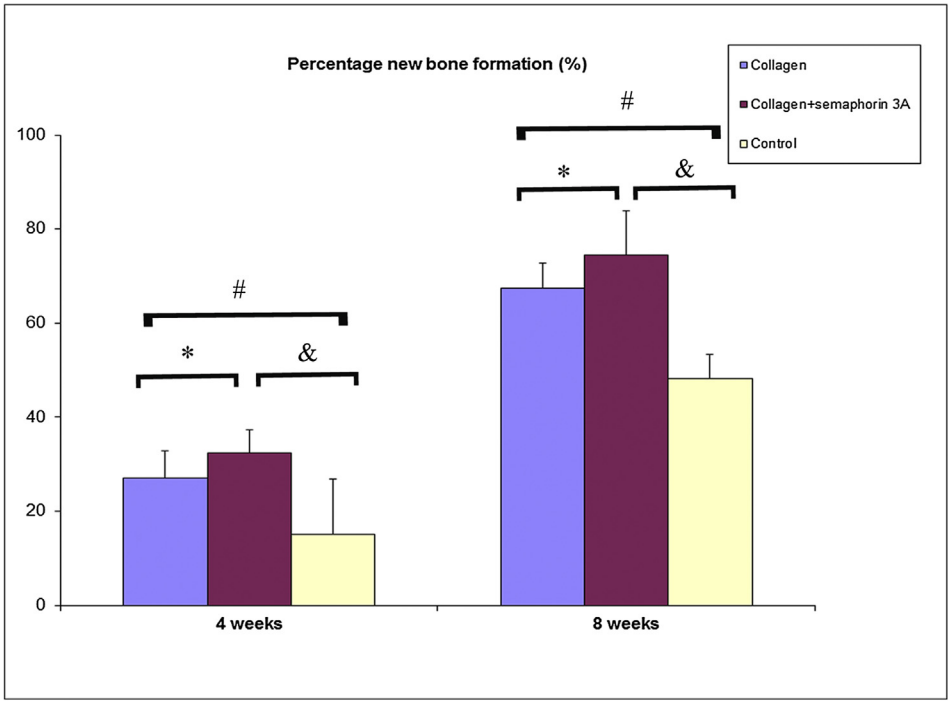

Fig. 4. Mean percentages of the newly formed bone in all groups at 4 and 8 weeks. *Significant difference between collagen group and collagen + semaphorin 3A group at 4 weeks ($p = 0.002$) and at 8 weeks ($p = 0.005$). # Significant difference between control group and collagen group at 4 weeks ($p = 0.0001$) and at 8 weeks ($p = 0.0001$). &Significant difference between control group and collagen + semaphorin 3A group at 4 weeks ($p = 0.0001$) and at 8 weeks ($p = 0.0001$).

collagen + semaphorin 3A group ($p = 0.0001$). At 8 weeks, the collagen group showed a significantly lower percentage of bone formation compared to the collagen + semaphorin 3A group ($p = 0.005$) (Fig. 4).

3.3. TEM evaluation

At 4 weeks, the collagen + semaphorin 3A group displayed signs of enhanced proliferation and early callus formation. Osteoblasts were observed to form groups similar to cartilaginous tissue, and collagen fibers were typically organized, compatible with the pattern of trabecular bone along with osteocytes. In the 4-week control group, collagen fibers were disarrayed and reparative connective tissue components with vascular elements were dominant. Components of the inflammation period, large vacuoles and free blood cells, were observed in this group. In the 4-week collagen group, although some granulation tissue was present, reparative tissue was more common with organized collagen fibers, vascular components and clusters of osteoblasts (Fig. 5).

At 8 weeks, complete bone formation and enhanced mineralization was prominent in the collagen + semaphorin 3A group. Mineralized bone matrix was dominant, and in some areas osteoblast synthesizing osteoid were observed. In the 8-week control group, primary bone tissue was observed with many osteoclastic cells. In the 8-week collagen group, trabecular bone formation with a lamellar structure was detected, yet mineralization was not evident (Fig. 6).

3.4. Immunohistochemical staining

Semi-quantitative results of the immunohistochemical staining with Runx2, RANK, RANKL, OPG, sp7 osterix, β-catenin and ATF4 are given in Table 1. Representative sections for each antibody are shown in Figs. 7 and 8.

Negative immunostaining of RANKL was observed in the collagen + semaphorin 3A group both at 4 weeks and at 8 weeks.

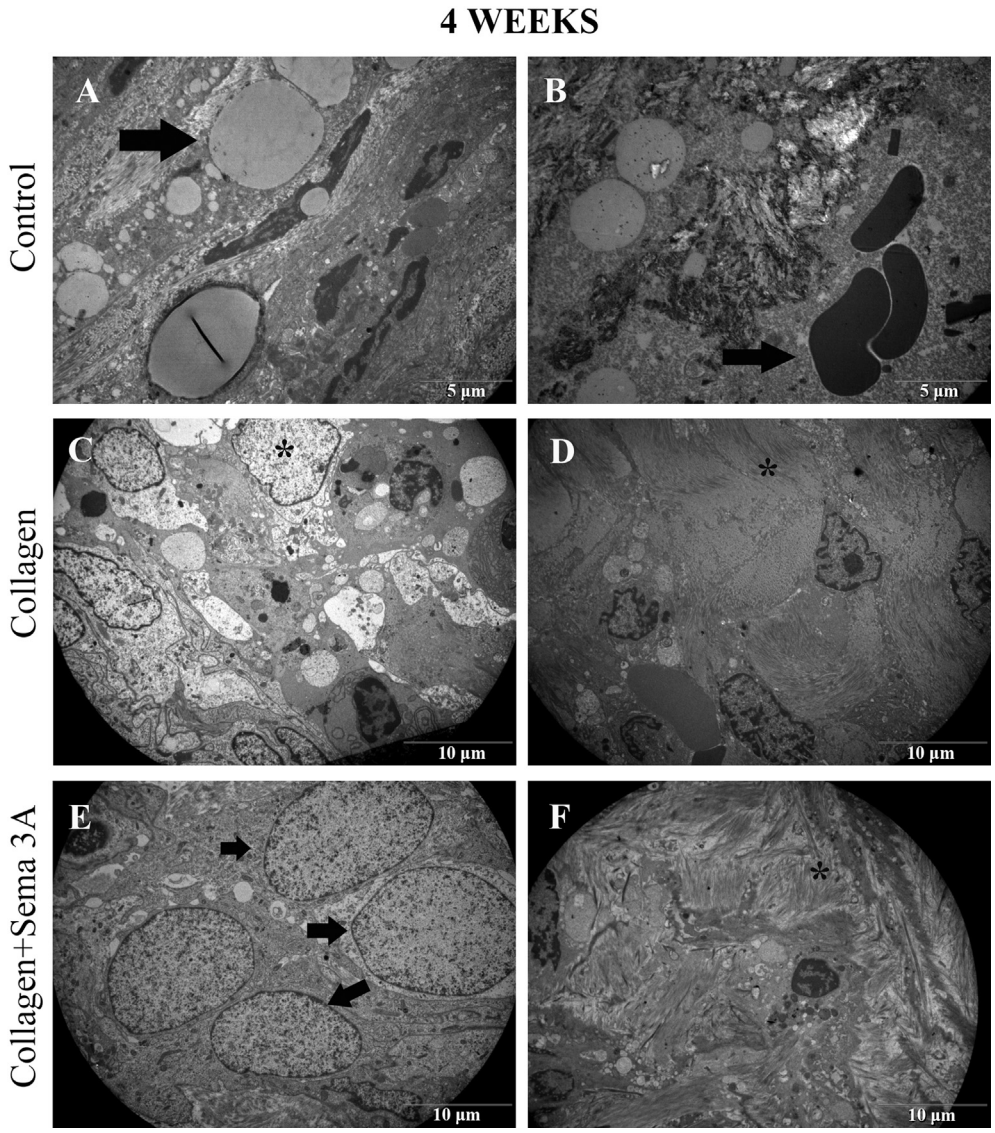

Figure 5. (A, B) Representative TEM images of control group at 4 weeks. Reparative connective tissue components, large vacuoles and free blood cells, indicated by arrows, are observed. (C, D) Representative TEM images of collagen group at 4 weeks. Asterisks indicate osteoblasts and collagen fibers. (E, F) Representative TEM image of collagen + semaphorin 3A (Sema3A) group at 4 weeks. Arrows indicate active osteoblasts gathering into clusters similar to cartilaginous tissue and asterisk indicates organized collagen fibers.

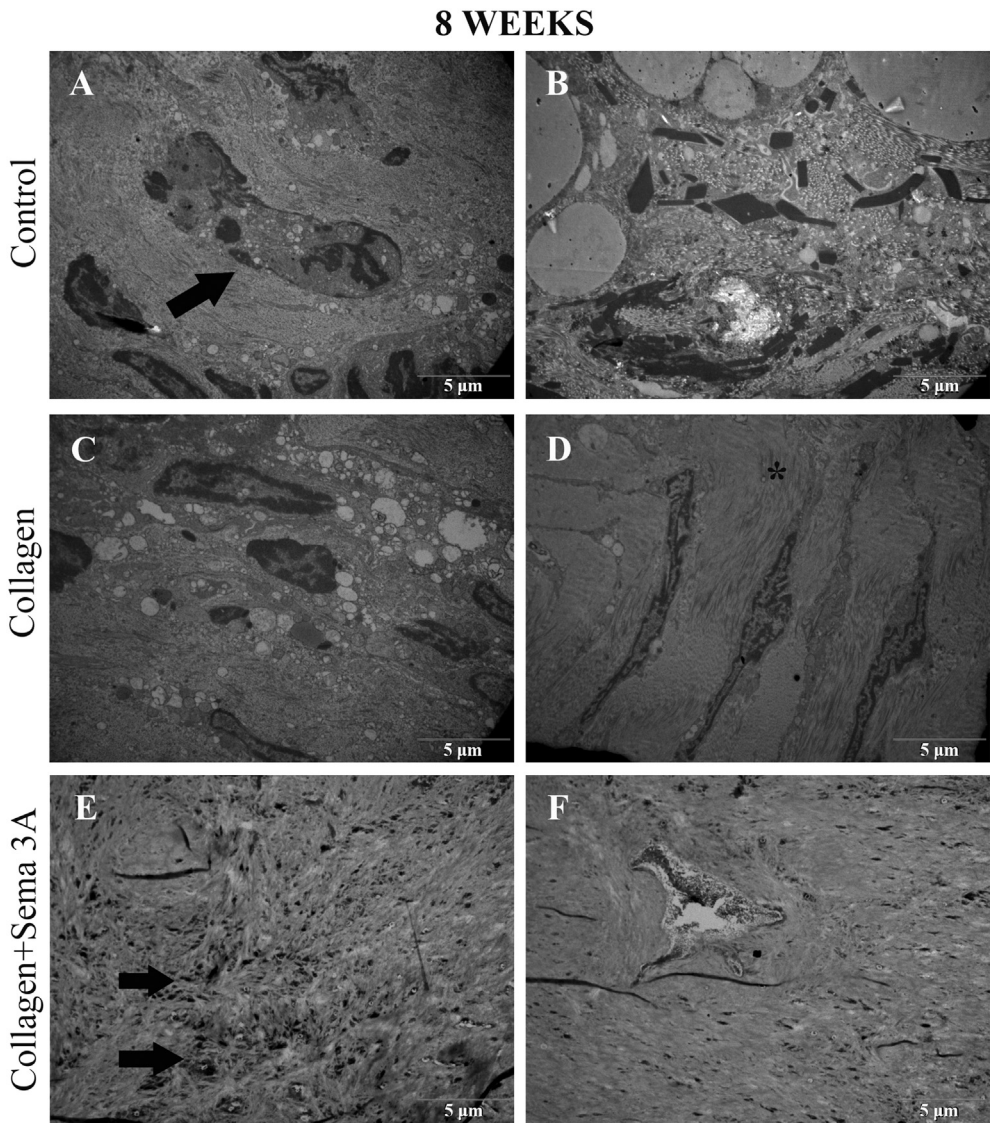

Fig. 6. (A, B) Representative TEM images of control group at 8 weeks. Arrow indicates an osteoclastic cell with resorption vacuoles. (C, D) Representative TEM images of collagen group at 8 weeks. Asterisks indicates trabecular bone formation without mature mineralization is observed. (E, F) Representative TEM images of collagen + semaphorin 3A (Sema3A) group at 8 weeks. Arrows indicate hydroxyapatite crystals dispersed in highly mineralized new bone.

In this group, negative immunostaining for RANK was detected at 4 weeks. Both the control and the collagen group showed positive immunostaining of RANK and RANKL at 4 and 8 weeks.

Slight OPG immunoreactivity was observed in all groups at 4 and 8 weeks, except in the 8-week control group, which showed negative immunostaining of OPG.

The strongest positive immunostaining of Runx2 was detected in the 4-week collagen + semaphorin 3A group. At 8 weeks, immunostaining with Runx2 was weak, both in the collagen and in the collagen + semaphorin 3A groups.

Immunostaining with β-catenin was more prominent in the collagen + semaphorin 3A group compared to other

Table 1
Semi-quantitative results of the immunohistochemical staining with Runx2, RANK, RANKL, OPG, sp7 osterix, β-catenin and ATF4 of the groups at 4 and 8 weeks.

	4 Weeks			8 Weeks		
	Control	Collagen	Collagen + Sema 3A	Control	Collagen	Collagen + Sema 3A
Runx2	Random +	++	+++	++	Faint +	Faint +
RANK	Diffuse++	+	–	In osteogenic foci ++	+	In lamellar area +
RANKL	+	Faint +	–	Peripheral +	Faint +	-
OPG	Faint and scarce +	Faint and scarce +	Faint +	–	Faint and scarce +	Faint +
SP7	Scarce +	Scarce +	Diffuse +	+	+±	+
β-catenin	±	+	++	–	Scarce ±	Scarce ±
ATF4	+++	+±	+±	++	+++	+++

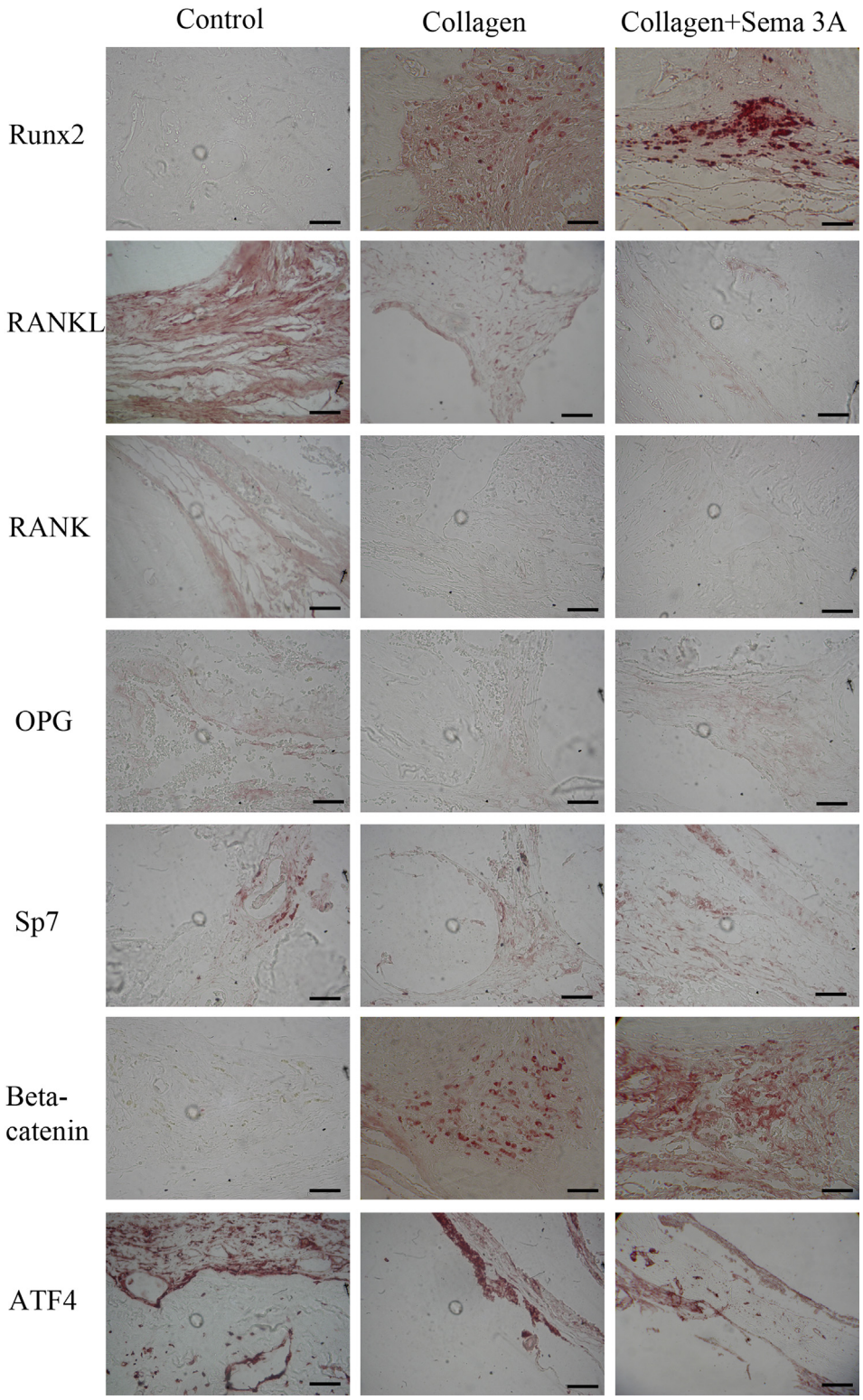

Fig. 7. Representative immunohistochemical staining images of the groups for each antibody reactivity at 4 weeks. In the collagen + semaphorin3A (Sema3A) group, stronger immunopositive staining is observed with markers of osteoblastic activity, Runx2, β-catenin and sp7, whereas RANK and RANKL staining is negative in this group. Scale bar = 50 μm, original magnification ×400.

study groups at 4 weeks. At 8 weeks, the collagen and the collagen + semaphorin 3A groups showed weak staining of β-catenin, and in the control group negative staining was present.

Immunostaining of ATF4 was positive in all groups at both 4 and 8 weeks. Immunostaining of sp7 was weak in all groups, yet staining was relatively more diffuse in the 4-week collagen + semaphorin group and stronger the 8-week collagen group.

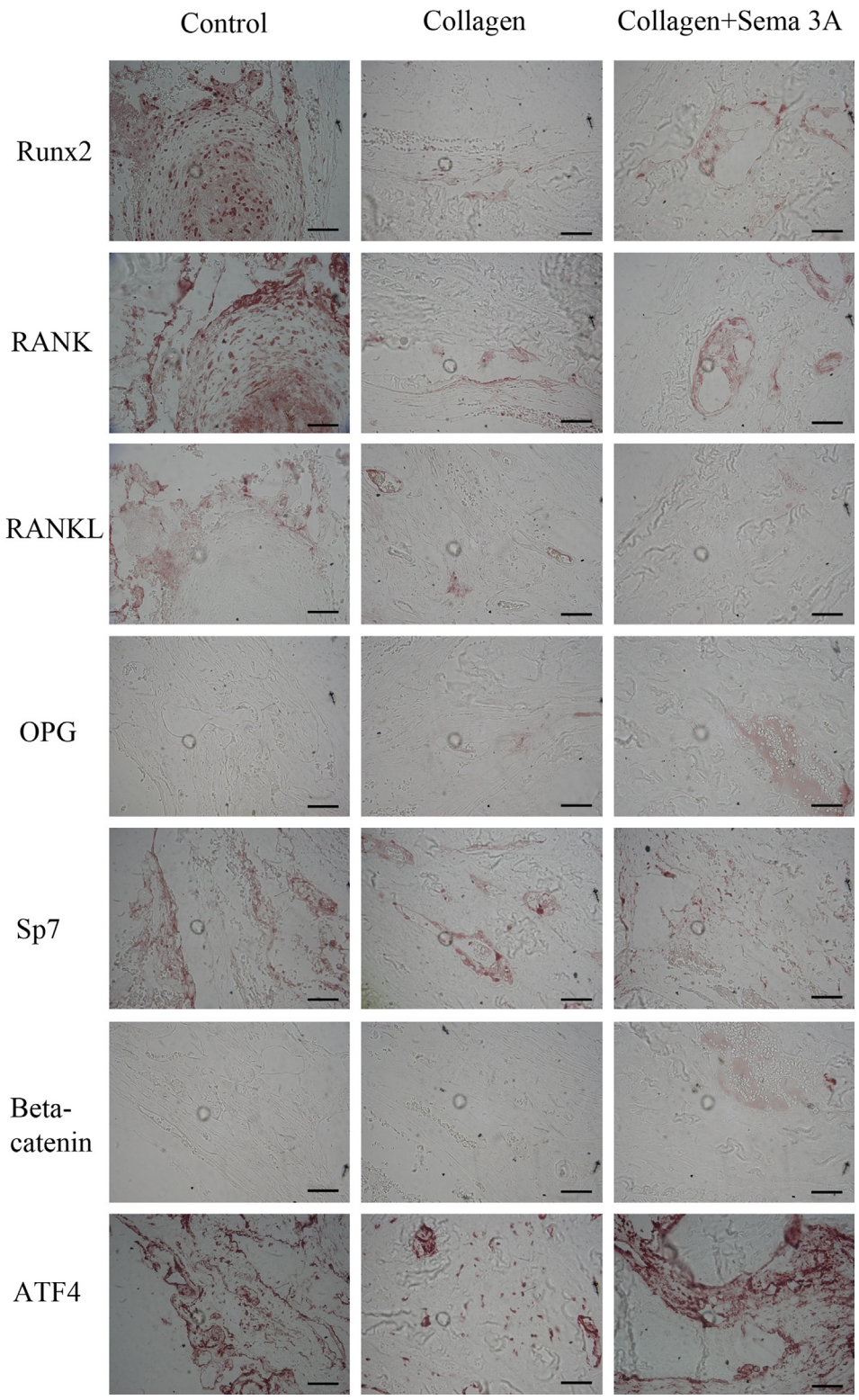

Fig. 8. Representative immunohistochemical staining images of the groups for each antibody reactivity at 8 weeks. In collagen + semaphorin 3A (Sema3A) group, RANKL staining is still negative and as bone maturation is complete, immunoreactivity with osteoblastic bone markers, Runx2 and β-catenin, has become weaker. Scale bar = 50 μm, original magnification ×400.

4. Discussion

In this study, the effects of locally applied semaphorin 3A on new bone formation were evaluated in an experimental rat model. It has been reported that semaphorin 3A exerts an osteoprotective effect by both suppressing osteoclastic bone resorption and increasing osteoblastic bone formation (Hayashi et al., 2012). Semaphorin 3A expression was found abundantly in bone, and

semaphoring-deficient mice had a low bone mass due to decreased bone formation (Fukuda et al., 2013).

Semaphorin 3A, a secreted type of semaphorin, is an axonal chemo repellent that has an important role in axon guidance during neural development and causes the inhibition of neurite outgrowth (Goshima et al., 2000). Bone tissue is known to be densely innervated, and recent evidence indicates a neural control of bone metabolism. Gomez et al. (2005) reported that semaphorin 3A signaling is present in bone and that this signaling precedes or coincides with the invasion of bone by blood vessels and nerve fibers. It is suggested that sensory nerves have an essential role in bone remodeling processes and that semaphorin 3A regulates bone remodeling, not directly by acting on osteoblasts but indirectly by modulating sensory nerve development (Togari et al., 2000; Fukuda et al., 2013).

The osteoprotective effects of semaphorin 3A have been reported in numerous studies. Intravenous semaphorin 3A administration in mice was shown to increase bone volume and to prevent bone loss induced by ovariectomy (Hayashi et al., 2012). Recently, semaphorin 3A have been used to increase the osteogenic differentiation of osteoblasts and to improve the osteointegration of titanium implants in vitro and in rat models (Fang et al., 2014, 2016; Li et al., 2017) Semaphorin 3A is shown to improve the osteogenesis ability of adipose mesenchmal stem cells, and semaphorin 3A-modified stem cells were shown to promote the repair of critical-size calvarial defects in a rat model (Fang et al., 2016; Liu et al., 2016).

Based on recent literature findings, our study was designed to examine the effects of semaphorin 3A on bone remodeling and to evaluate its role in the regeneration process of critical-size defects. For this purpose, semaphorin 3A was applied locally to a critical-size calvarial defect using type 1 collagen matrix as its carrier in a rat experimental model. Previous studies have investigated the effects of locally applied (by local injection) semaphorin 3A in a bone regeneration model of cortical bone defect induced by drill in the proximal femurs of mice and in the fracture healing induced on the proximal tibia of rats (Hayashi et al., 2012; Li et al., 2015). Both studies reported positive results in regard to the therapeutic potential of semaphorin 3A. Yet there are no previous studies conducted using a carrier matrix in a calvarial rat model.

In the experimental studies, a calvarial defect model is frequently used for the investigation of bone regeneration, because it does not require fixation and it represents intramembranous bone formation (Spicer et al., 2012). A critical-size defect can be described as the smallest intra-osseous wound which does not heal spontaneously during the lifetime of the animal. In rats, the dimension of the critical defect size is still controversial (Gomes; Fernandes, 2011). Bosch et al. (1998) reported that a 5-mm defect was unable to heal spontaneously up to 12 months after the surgery. In the present study, 5-mm critical-sized defects were created in the calvaria of rats. The suitability of this defect size was confirmed by the lack of complete bone regeneration after 8 weeks in the control group in our experiment.

In the micro-CT assessment, the collagen + semaphorin 3A group displayed the highest amount of new bone formation both at 4 weeks and at 8 weeks. The collagen group also showed increased bone volume compared to the control group at both weeks 4 and 8. The bone percentage values and the images taken from the representative specimens confirm the positive effect of semaphorin 3A on bone regeneration. Complete defect closure was observed in the semaphorin 3A-applied group at 8 weeks.

Histological specimens also demonstrate enhanced bone formation with semaphorin 3A. In the histological analysis with H&E staining, the collagen + semaphorin 3A group displayed increased ossification sites at 4 weeks, while in the other two groups fibrous tissue was dominant at 4 weeks. At 8 weeks, although ossification was increased in the control and collagen groups, the semaphorin 3A-applied group displayed nearly complete ossification of the same quality with the peripheral sound bone. TEM images confirmed enhanced proliferation at 4 weeks and mineralization at 8 weeks in the semaphorin 3A-applied group. Various studies have reported enhanced ossification with semaphorin 3A application using micro-CT and histological analysis (Hayashi et al., 2012; Li et al., 2015). The results of our study are in agreement with the available literature.

Immunohistochemical analysis in our study demonstrates the inhibitory effect of semaphorin 3A on osteoclasts. At 4 weeks, no reactivity was detected for both RANKL and RANK for the collagen + semaphorin group. At 8 weeks, there was still no reactivity for RANKL and only slight reactivity with RANK. Recent findings show that osteoclast differentiation is tightly regulated by osteoblasts through several different mechanisms. Semaphorin 3A produced by osteoblasts inhibits RANKL-induced osteoclast differentiation through the suppression of ITAM signals (Yamashita et al., 2012). Hayashi et al. (2012) reported that the binding of semaphorin 3A to its receptor Nrp1 inhibited RANKL-induced osteoclast differentiation by inhibiting ITAM and RhoA signaling pathways. Our findings also indicate that semaphorin 3A inhibits osteoclast formation and function by inhibiting RANKL.

The immunohistochemical results of our study reveal enhanced bone formation activity and increased osteoblastic markers in the collagen + semaphorin 3A group at 4 weeks. Enhanced immunoreactivity was observed for Runx2, β-catenin, sp7 and ATF4 in this group at 4 weeks. Runx2, which induces the differentiation of multipotent mesenchymal cells into immature osteoblasts and directs the formation of immature bone (Komori, 2010), was strongly expressed in this group. This finding implicates osteoinductivity in the early stages of osteoblast differentiation. Previous studies have also reported increased osteoblastic markers with semaphorin 3A application (Fang et al., 2014; Liu et al., 2015; Shen et al., 2015).

It is reported that semaphorin 3A and Nrp1 binding stimulated osteoblast differentiation through the canonical Wnt/β-catenin signaling pathway and that semaphorin 3A application increased nuclear β-catenin accumulation (Hayashi et al., 2012; Ma et al., 2016; Yoshida et al., 2016). In our study, the increased immunoreactivity for β-catenin detected in the collagen + semaphorin 3A group compared to other groups at 4 weeks is compatible with the findings of previous studies.

The weak immunoreactivity of OPG observed in semaphorin 3A-applied groups might be interpreted as evidence that the osteoprotective mechanisms of OPG and semaphorin differ and not dependent on each other. Accordingly, it is reported that conditioned medium from OPG-deficient mouse calvarial cells contains factors that inhibit osteoclast formation, one of them being semaphorin 3A (Hayashi et al., 2012).

In summary, the effect of semaphorin 3A on bone formation was evaluated using micro-CT, histology, histomorphometry, immunohistochemistry and TEM analysis. With all the assessment methods, locally applied semaphorin 3A was found to increase bone formation rate and to enhance the quantity and quality of the resulting new bone.

Collagen sponge is used both as a hemostatic agent and as a scaffold for bone tissue engineering, and it has been shown that it stimulates bone repair (Kim et al., 2013; Santos et al., 2015). The use of collagen sponge in a perforated cortical model promotes bone formation by acting as a scaffold for cells and by providing the space needed for bone growth (Shimoji et al., 2009). The findings of our study demonstrate that collagen sponge alone promotes bone healing, possibly due to its osteoconductive property and by acting as a scaffold.

The results of our study show that when semaphorin 3A is combined with the collagen matrix, bone regeneration is enhanced. Various carrier matrices have been used in a variety of drugs for various purposes. Use of hydrogels such as collagen and gelatin is a popular method of local drug delivery for bone applications (Shah et al., 2015). There are a few studies that report using a carrier matrix for semaphorin 3A application. One such study reports using chitosan to wrap semaphorin 3A and then connect it to a micro-arc oxided titanium implant surface. The authors of the study reported improved osteogenic differentiation of osteoblasts and suggested that chitosan film might be an ideal carrier of semaphorin 3A (Fang et al., 2014). In another study, collagen sponge coated by nanoparticles of beta-tricalcium phosphate was used to carry semaphorin 3A onto the pulp exposure site in an investigational model of direct pulp capping (Yoshida et al., 2016). In our study, enhanced bone formation rate at 4 weeks and prolonged RANKL inhibition until 8 weeks indicate that the physiological effects of semaphorin 3A continue for a long time and do not dissipate rapidly after application. These findings show that collagen sponge might be a suitable carrier matrix for semaphorin 3A. They also point out that a single dose application might be enough to promote bone formation. More studies are required to determine the ideal route of application, dosage and dose intervals for semaphorin 3A.

5. Conclusion

The results of this study indicate that semaphorin 3A has a favorable effect on bone regeneration. All the assessment methods used in this study demonstrate that locally applied semaphorin 3A enhances new bone formation by increasing osteoblastic activity and inhibiting osteoclasts. Thus, it can be suggested that semaphorin 3A may be used as a therapeutic agent for the treatment of bone defects and various bone disorders, including osteoporosis.

Conflicts of interest

The authors declare no conflict of interest.

Acknowledgement

This study was supported by the 3001- Research and Development Projects Funding Program of The Scientific and Technological Research Council of Turkey (TÜBİTAK), Turkey (Project No: 214S554).

References

Behar O, Golden JA, Mashimo H, Schoen FJ, Fishman MC: Semaphorin III is needed for normal patterning and growth of nerves, bones and heart. Nature 383(6600): 525–528, 1996
Bosch C, Melsen B, Vargervik K: Importance of the critical-size bone defect in testing bone-regenerating materials. J Craniofac Surg 9(4): 310–316, 1998
Epstein JA, Aghajanian H, Singh MK: Semaphorin signaling in cardiovascular development. Cell Metab 21(2): 163–173, 2015
Fang K, Song W, Wang L, Jia S, Wei H, Ren S, Xu X, Song Y: Immobilization of chitosan film containing semaphorin 3A onto a microarc oxidized titanium implant surface via silane reaction to improve MG63 osteogenic differentiation. Int J Nanomed 9: 4649–4657, 2014
Fang K, Song W, Wang L, Xu X, Tan N, Zhang S, Wei H, Song Y: Semaphorin 3A-modified adipose-derived stem cell sheet may improve osseointegration in a type 2 diabetes mellitus rat model. Mol Med Rep 14(3): 2449–2456, 2016
Fukuda T, Takeda S, Xu R, Ochi H, Sunamura S, Sato T, Shibata S, Yoshida Y, Gu Z, Kimura A, Ma C, Xu C, Bando W, Fujita K, Shinomiya K, Hirai T, Asou Y, Enomoto M, Okano H, Okawa A, Itoh H: Sema3A regulates bone-mass accrual through sensory innervations. Nature 497(7450): 490–493, 2013
García-Gareta E, Coathup MJ, Blunn GW: Osteoinduction of bone grafting materials for bone repair and regeneration. Bone 81: 112–121, 2015
Gomes PS, Fernandes MH: Rodent models in bone-related research: the relevance of calvarial defects in the assessment of bone regeneration strategies. Lab Anim 45(1): 14–24, 2011
Gomez C, Burt-Pichat B, Mallein-Gerin F, Merle B, Delmas PD, Skerry TM, Vico L, Malaval L, Chenu C: Expression of semaphorin-3A and its receptors in endochondral ossification: potential role in skeletal development and innervation. Dev Dyn 234(2): 393–403, 2005
Goshima Y, Sasaki Y, Nakayama T, Ito T, Kimura T: Functions of semaphorins in axon guidance and neuronal regeneration. Jpn J Pharmacol 82(4): 273–279, 2000
Harre U, Schett G: Bone research in 2012: the ups and downs of bone in health and rheumatic disease. Nat Rev Rheumatol 9(2): 67–68, 2013
Hayashi M, Nakashima T, Taniguchi M, Kodama T, Kumanogoh A, Takayanagi H: Osteoprotection by semaphorin 3A. Nature 485(7396): 69–74, 2012
Jongbloets BC, Pasterkamp RJ: Semaphorin signalling during development. Development 141(17): 3292–3297, 2014
Kang S, Kumanogoh A: Semaphorins in bone development, homeostasis, and disease. Semin Cell Dev Biol 24(3): 163–171, 2013
Kim BS, Kim JS, Lee J: Improvements of osteoblast adhesion, proliferation, and differentiation in vitro via fibrin network formation in collagen sponge scaffold. J Biomed Mater Res A 101(9): 2661–2666, 2013
Komori T: Regulation of osteoblast differentiation by Runx2. Adv Exp Med Biol 658: 43–49, 2010
Li Y, Yang L, He S, Hu J: The effect of semaphorin 3A on fracture healing in osteoporotic rats. J Orthop Sci 20(6): 1114–1121, 2015
Li Y, He D, Liu B, Hu J: SEMA3A suspended in Matrigel improves titanium implant fixation in ovariectomized rats. J Biomed Mater Res B Appl Biomater 105(7): 2060–2065, 2017
Liu F, Shen W, Qiu H, Hu X, Zhang C, Chu T: Prostate cancer cells induce osteoblastic differentiation via semaphorin 3A. Prostate 75(4): 370–380, 2015
Liu X, Tan N, Zhou Y, Zhou X, Chen H, Wei H, Chen J, Xu X, Zhang S, Yang G, Song Y: Semaphorin 3A shifts adipose mesenchymal stem cells towards osteogenic phenotype and promotes bone regeneration in vivo. Stem Cells Int 2016, 2016 2545214
Ma X, Lv J, Sun X, Ma J, Xing G, Wang Y, Sun L, Wang J, Li F, Li Y, Zhao Z: Naringin ameliorates bone loss induced by sciatic neurectomy and increases semaphorin 3A expression in denervated bone. Sci Rep 6: 24562, 2016
Negishi-Koga T, Takayanagi H: Bone cell communication factors and semaphorins. BoneKEy Rep 1: 183, 2012
Roth L, Koncina E, Satkauskas S, Cremel G, Aunis D, Bagnard D: The many faces of semaphorins: from development to pathology. Cell Mol Life Sci 66(4): 649–666, 2009
Santos Tde S, Abuna RP, Almeida AL, Beloti MM, Rosa AL: Effect of collagen sponge and fibrin glue on bone repair. J Appl Oral Sci 23(6): 623–628, 2015
Shah SR, Werlang CA, Kasper FK, Mikos AG: Novel applications of statins for bone regeneration. Natl Sci Rev 2(1): 85–99, 2015
Shen WW, Chen WG, Liu FZ, Hu X, Wang HK, Zhang Y, Chu TW: Breast cancer cells promote osteoblastic differentiation via Sema 3A signaling pathway in vitro. Int J Clin Exp Pathol 8(2): 1584–1593, 2015
Shimoji S, Miyaji H, Sugaya T, Tsuji H, Hongo T, Nakatsuka M, Zaman KU, Kawanami M: Bone perforation and placement of collagen sponge facilitate bone augmentation. J Periodontol 80(3): 505–511, 2009
Spicer PP, Kretlow JD, Young S, Jansen JA, Kasper FK, Mikos AG: Evaluation of bone regeneration using the rat critical size calvarial defect. Nat Protoc 7(10): 1918–1929, 2012
Stancoven BW, Lee J, Dixon DR, McPherson 3rd JC, Bisch FC, Wikesjö UM, Susin C: Effect of bone morphogenetic protein-2, demineralized bone matrix and systemic parathyroid hormone (1-34) on local bone formation in a rat calvaria critical-size defect model. J Periodontal Res 48(2): 243–251, 2013
Togari A, Mogi M, Arai M, Yamamoto S, Koshihara Y: Expression of mRNA for axon guidance molecules, such as semaphorin-III, netrins and neurotrophins, in human osteoblasts and osteoclasts. Brain Res 878(1–2): 204–209, 2000
Verlinden L, Vanderschueren D, Verstuyf A: Semaphorin signaling in bone. Mol Cell Endocrinol 432: 66–74, 2016
Xu R: Semaphorin 3A: a new player in bone remodeling. Cell Adh Migr 8(1): 5–10, 2014
Yamashita T, Takahashi N, Udagawa N: New roles of osteoblasts involved in osteoclast differentiation. World J Orthop 3(11): 175–181, 2012
Yazdani U, Terman JR: The semaphorins. Genome Biol 7(3): 211, 2006
Yoshida S, Wada N, Hasegawa D, Miyaji H, Mitarai H, Tomokiyo A, Hamano S, Maeda H: Semaphorin 3A induces odontoblastic phenotype in dental pulp stem cells. J Dent Res 95(11): 1282–1290, 2016
Zaidi M, Iqbal J: Translational medicine: double protection for weakened bones. Nature 485(7396): 47–48, 2012
Zhang L, Zhang L, Mao Z, Tang P: Semaphorin 3A: an association between traumatic brain injury and enhanced osteogenesis. Med Hypotheses 81(4): 713–714, 2013